Improving Cell-Free Massive MIMO Through Channel Map-Based Angle Domain Multiple Access

Shuaifei Chen[1,2], Cheng-Xiang Wang[2,1*], Junling Li[2,1], Chen Huang[1,2*], Hengtai Chang[3], and Yunfei Chen[4]
[1]Purple Mountain Laboratories, Nanjing 211111, China.
[2]National Mobile Communications Research Laboratory, School of Information Science and Engineering
Southeast University, Nanjing 211189, China.
[3]School of Information Science and Engineering, Shandong University, Qingdao 266237, China.
[4]Department of Engineering, University of Durham, DH1 3LE Durham, U.K.
*Corresponding Authors: Cheng-Xiang Wang and Chen Huang
Emails: {shuaifeichen, chxwang, junlingli}@seu.edu.cn, huangchen@pmlabs.com.cn, changht@sdu.edu.cn,
yunfei.chen@durham.ac.uk

ICC 2025 - IEEE International Conference on Communications | 979-8-3315-0521-9/25/$31.00 ©2025 IEEE | DOI: 10.1109/ICC52391.2025.11161836

***Abstract*—Cell-free (CF) massive multiple-input multiple-output (M-MIMO) provides an almost uniformly high data rate for all user equipment (UE) through multiple access points (APs), with a non-negligible signal processing burden. Angle domain transmission and channel maps promise to alleviate this burden by reducing channel dimensions in the angle domain and providing *a priori* channel information, respectively. In this paper, we propose a channel map-based angle domain multiple access scheme for uplink CF M-MIMO communications. First, we propose a two-stage data reception and pilot assignment scheme constituting receive combining and large-scale fading decoding (LSFD) to reduce overall interference and maximize spectral efficiency (SE). Furthermore, we construct two channel map-based transmission mechanisms by wielding different levels of channel information, where a tailored data reception scheme with a newly derived SE upper bound is also proposed for quantitative evaluation. Simulation results show that the proposed schemes outperform both their space domain alternatives and those without using channel maps in terms of SE.**

***Index Terms*—Angle domain, cell-free massive MIMO, channel map, distributed processing, multiple access.**

I. Introduction

The sixth-generation (6G) mobile communications are envisioned as an era of "global coverage, all spectra, full applications, all senses, all digital, and strong security" [1]. As one of the most promising enabling technologies, CF M-MIMO has garnered extensive attention from both academia and industry recently [2]. As illustrated in Fig. 1, CF M-MIMO allows each UE to be served by multiple APs coordinated by a central processing unit (CPU), inheriting proven signal processing techniques from cellular M-MIMO by equipping multiple antennas at each AP and enhancing so-called *macro-diversity gain* with reduced average AP-UE distances.

The distributed nature of CF M-MIMO introduces new opportunities and challenges for multiple access design. By only exploiting large-scale fading (LSF) coefficients, CF M-MIMO features a two-stage signal processing approach called LSFD [3], which achieves comparable SE to the centralized approach but with lower computational complexity. Pilot assignment design poses additional challenges due to the combinatorial nature of serving each UE with multiple APs. Common methods include random and greedy assignments [2]. More sophisticated

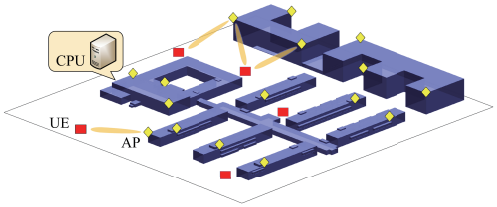

Fig. 1. Considered CF M-MIMO system.

methods, such as graphic [4] and genetic algorithm-based [5] approaches, can enhance assignment performance but increase complexity. Although these methods excel in specific scenarios, they focus on the space domain, while the actual data streams propagate as beams in the angle domain. Additionally, they often overlook environment-related channel state information (CSI) that could aid transmission.

Angle domain channel models have been effectively applied in M-MIMO scenarios [6], with successes in channel estimation [7], unmanned aerial vehicle (UAV) communications [8], etc. They reduce processing complexity by lowering the channel dimension [9] while maintaining comparable accuracy to space domain models like the pioneering 6G pervasive channel model (6GPCM) [10], [11]. Additionally, the natural angle domain sparsity can be used for interference suppression in large CF M-MIMO systems. Transmission performance can also be improved using refined CSI that reflects real-world environments. Channel maps offer an emerging tool to describe environment-related characteristics within specific areas, which use geographical inputs to produce desired CSI, such as channel gains and even complete channel coefficients [12]. Thus, they enhance transmission quality and reduce processing complexity by providing *a priori* environment-related CSI, enabling effective beamforming [13], UAV trajectory planning [14], etc. However, to the best of our knowledge, channel map-aided angle domain transmission has not been explored in the CF literature.

To fill the above gaps, in this paper we propose a channel map-based angle domain multiple access scheme for uplink CF M-MIMO. We propose a two-stage data reception scheme incorporating receive combining and LSFD design and a pilot assignment scheme using the angle domain UE similarity based on the derived criterion. We also construct two channel

map-based transmission mechanisms featuring a tailored data reception scheme with a newly derived upper-bound SE expression. The proposed schemes are compared with their space domain alternatives and the schemes without channel maps for effectiveness validation.

The rest of this paper is organized as follows. Section II introduces the considered system model. Section III details the angle domain multiple access transmission design. Section IV elaborates on the channel map-based transmission design with a tailored data reception scheme. Simulation results are provided in Section V. Finally, Section VI draws the conclusions.

II. System Model

As illustrated in Fig. 1, we consider a user-centric CF M-MIMO system consisting of L APs and K single-antenna UE. We assume that each AP is elevated and equipped with a uniform linear array (ULA) with N half-wavelength-spaced omnidirectional antennas. Each UE is surrounded by dense scatterers and served by multiple APs coordinated via a CPU for fronthaul connections. We let $\mathcal{D}_l \subset \{1,\dots,K\}$ denote the set of UE served by AP l.

We adopt the block fading model with standard time division duplex operation, where each time-frequency resource is divided into multiple coherence blocks so that the pilot sequences and payload data can be assumed to transmit in each block with fixed channel coefficients. Each coherence block of τ_{c} channel uses is separated into two segments, where τ_{p} channel uses are dedicated to pilot transmission and channel estimation, and the remaining $\tau_{\mathrm{u}} = \tau_{\mathrm{c}} - \tau_{\mathrm{p}}$ channel uses are used for the uplink payload data transmission.

We consider a narrowband system operating in the angle domain, where the space domain channel vector between AP l and UE k, i.e., $\mathbf{h}_{kl} \in \mathbb{C}^N$, can be represented by its angle domain channel vector $\mathbf{g}_{kl} \in \mathbb{C}^N$. More precisely, we have [8]

$$\mathbf{h}_{kl} = \mathbf{U}\mathbf{g}_{kl} \in \mathbb{C}^N \tag{1}$$

where $\mathbf{U} \in \mathbb{C}^{N\times N}$ is a deterministic matrix satisfying $\mathbf{U}^{\mathrm{H}}\mathbf{U} = N\mathbf{I}_N$, of which the columns are the sampled steering vectors of the N angular beams covering the entire angle domain. According to the multidimensional central limit theorem, the space domain channel $\mathbf{h}_{kl}$ can be drawn from a simplified instance of the 6GPCM [10] as

$$\mathbf{h}_{kl} = \mathbf{h}^{\mathrm{L}}_{kl} e^{\jmath\phi_{kl}} + \mathbf{h}^{\mathrm{N}}_{kl} = \mathbf{U}\mathbf{g}^{\mathrm{L}}_{kl} e^{\jmath\phi_{kl}} + \mathbf{U}\mathbf{g}^{\mathrm{N}}_{kl} \tag{2}$$

when the number of multipath components between AP l and UE k tends to be infinite. The deterministic line-of-sight (LoS) component is denoted by $\mathbf{h}^{\mathrm{L}}_{kl} \in \mathbb{C}^N$ with $\beta^{\mathrm{L}}_{kl} = \frac{1}{N}(\mathbf{h}^{\mathrm{L}}_{kl})^{\mathrm{H}}\mathbf{h}^{\mathrm{L}}_{kl}$ and $\mathbf{g}^{\mathrm{L}}_{kl} \in \mathbb{C}^N$ being its LSF coefficient and angle domain representative, respectively. The phase-shift of the LoS component, i.e., $\phi_{kl} \sim \mathcal{U}[-\pi,\pi]$, is uniformly distributed. The stochastic non-LoS (NLoS) components are represented by $\mathbf{h}^{\mathrm{N}}_{kl} \sim \mathcal{N}_{\mathbb{C}}(\mathbf{0}, \mathbf{R}^{\mathrm{N}}_{kl})$ with $\mathbf{R}^{\mathrm{N}}_{kl} = \mathbb{E}\{\mathbf{h}^{\mathrm{N}}_{kl}(\mathbf{h}^{\mathrm{N}}_{kl})^{\mathrm{H}}\} \in \mathbb{C}^{N\times N}$, $\beta^{\mathrm{N}}_{kl} = \frac{1}{N}\mathrm{tr}(\mathbf{R}^{\mathrm{N}}_{kl})$, and $\mathbf{g}^{\mathrm{N}}_{kl} \in \mathbb{C}^N$ being the corresponding covariance matrix, LSF coefficient, and angle domain representative, respectively. Note that the phase-shift ϕ_{kl} varies at the same pace as $\mathbf{h}^{\mathrm{L}}_{kl}$ and is assumed to be independent and identically distributed in each coherence block. Accordingly, the covariance matrix of $\mathbf{h}_{kl}$ is obtained as $\mathbf{R}_{kl} = \mathbb{E}\{\mathbf{h}_{kl}\mathbf{h}^{\mathrm{H}}_{kl}\} = \mathbf{h}^{\mathrm{L}}_{kl}(\mathbf{h}^{\mathrm{L}}_{kl})^{\mathrm{H}} + \mathbf{R}^{\mathrm{N}}_{kl}$ with $\beta_{kl} = \frac{1}{N}\mathrm{tr}(\mathbf{R}_{kl})$ being the corresponding LSF coefficient. Additionally, $\mathbf{\Omega}_{kl} = \mathbb{E}\{\mathbf{g}_{kl}\mathbf{g}^{\mathrm{H}}_{kl}\} = \frac{1}{N^2}\mathbf{U}^{\mathrm{H}}\mathbf{R}_{kl}\mathbf{U} = \mathbf{g}^{\mathrm{L}}_{kl}(\mathbf{g}^{\mathrm{L}}_{kl})^{\mathrm{H}} + \mathbf{\Omega}^{\mathrm{N}}_{kl} \in \mathbb{C}^{N\times N}$ is the covariance matrix of $\mathbf{g}_{kl}$ with $\mathbf{\Omega}^{\mathrm{N}}_{kl} = \mathbb{E}\{\mathbf{g}^{\mathrm{N}}_{kl}(\mathbf{g}^{\mathrm{N}}_{kl})^{\mathrm{H}}\} \in \mathbb{C}^{N\times N}$.

The LSF coefficient β_{kl} is allocated to the LoS and NLoS components by the location-related Rician K-factor $\kappa_{kl} = p^{\mathrm{L}}_{kl} \cdot 10^{1.3-0.003 d_{kl}}$ [15] in linear scale as

$$\beta^{\mathrm{L}}_{kl} = \frac{\kappa_{kl}}{\kappa_{kl}+1}\beta_{kl}, \quad \beta^{\mathrm{N}}_{kl} = \frac{1}{\kappa_{kl}+1}\beta_{kl} \tag{3}$$

where $d_{kl} = \|\mathbf{c}^{\mathrm{ap}}_l - \mathbf{c}^{\mathrm{ue}}_k\|^2 \in \mathbb{R}$ is the distance between AP l and UE k determined by their available three-dimensional location vectors $\mathbf{c}^{\mathrm{ap}}_l \in \mathbb{R}^3$ and $\mathbf{c}^{\mathrm{ue}}_k \in \mathbb{R}^3$ with $p^{\mathrm{L}}_{kl} \in \{0,1\}$ being the corresponding LoS probability. More precisely, $p^{\mathrm{L}}_{kl} = 1$ indicates the existence of the LoS component and $p^{\mathrm{L}}_{kl} = 0$ otherwise.

III. Angle Domain Multiple Access Transmission

A. Channel Estimation via Pilot Transmission

During the uplink pilot phase, each AP locally performs channel estimation based on the received uplink pilots transmitted from all UE. Each UE is assigned a τ_{p}-length pilot sequence from an orthogonal pilot set with a cardinality of τ_{p}. The pilots must be shared between UE since it is likely to have $\tau_{\mathrm{p}} \ll K$ in practice. We denote by ι_k the pilot index assigned to UE k and $\mathcal{S}_{\iota_k}$ the set of UE sharing pilot ι_k.

When UE transmit their pilots, the received pilot signal $\mathbf{y}^{\mathrm{p}}_{\iota_k l} \in \mathbb{C}^N$ at AP l after despreading with pilot ι_k is

$$\mathbf{y}^{\mathrm{p}}_{\iota_k l} = \sqrt{\tau_{\mathrm{p}} p_{\mathrm{p}}}\mathbf{U}\mathbf{g}_{kl} + \sqrt{\tau_{\mathrm{p}} p_{\mathrm{p}}}\sum\nolimits_{i\in\mathcal{S}_{\iota_k}\setminus\{k\}} \mathbf{U}\mathbf{g}_{il} + \mathbf{n}_l \tag{4}$$

where p_{p} represents the transmit power for pilots and $\mathbf{n}_l \sim \mathcal{N}_{\mathbb{C}}(\mathbf{0}, \sigma^2\mathbf{I}_N)$ represents the receiver noise with power σ^2.

If the deterministic LoS component $\mathbf{h}^{\mathrm{L}}_{kl}$ is available at AP l while the phase-shift ϕ_{kl} is not, the *linear minimum mean-squared-error (MMSE)* estimate of $\mathbf{g}_{kl}$ can be derived as

$$\widehat{\mathbf{g}}_{kl} = \sqrt{\tau_{\mathrm{p}} p_{\mathrm{p}}}\mathbf{\Omega}_{kl}\mathbf{U}^{\mathrm{H}}\mathbf{\Psi}^{-1}_{\iota_k l}\mathbf{y}^{\mathrm{p}}_{\iota_k l} \tag{5}$$

where $\mathbf{\Psi}_{\iota_k l} = \mathbb{E}\{\mathbf{y}^{\mathrm{p}}_{\iota_k l}(\mathbf{y}^{\mathrm{p}}_{\iota_k l})^{\mathrm{H}}\} = \tau_{\mathrm{p}} p_{\mathrm{p}}\sum_{i\in\mathcal{S}_{\iota_k}}\mathbf{U}\mathbf{\Omega}_{il}\mathbf{U}^{\mathrm{H}} + \sigma^2\mathbf{I}_N$ is the correlation matrix of $\mathbf{y}^{\mathrm{p}}_{\iota_k l}$ in (4). Due to the pilot sharing among UE, $\mathbf{\Psi}_{\iota_k l}$ contains the statistical CSI of all UE in $\mathcal{S}_{\iota_k}$, which induces the so-called *pilot contamination* and thus degrades the channel estimation quality. The angle domain channel estimate $\widehat{\mathbf{g}}_{kl}$ and its estimation error $\widetilde{\mathbf{g}}_{kl} = \mathbf{g}_{kl} - \widehat{\mathbf{g}}_{kl}$ are uncorrelated random variables with

$$\mathbb{E}\{\widehat{\mathbf{g}}_{kl}\} = \mathbf{0}, \quad \mathsf{Cov}\{\widehat{\mathbf{g}}_{kl}\} = \mathbf{\Omega}_{kl} - \mathbf{\Xi}_{kl} \tag{6}$$

$$\mathbb{E}\{\widetilde{\mathbf{g}}_{kl}\} = \mathbf{0}, \quad \mathsf{Cov}\{\widetilde{\mathbf{g}}_{kl}\} = \mathbf{\Xi}_{kl} \tag{7}$$

where $\mathbf{\Xi}_{kl} = \mathbf{\Omega}_{kl} - \tau_{\mathrm{p}} p_{\mathrm{p}}\mathbf{\Omega}_{kl}\mathbf{U}^{\mathrm{H}}\mathbf{\Psi}^{-1}_{\iota_k l}\mathbf{U}\mathbf{\Omega}_{kl}$. The linear MMSE estimate of $\mathbf{h}_{kl}$ can be represented as $\widehat{\mathbf{h}}_{kl} = \mathbf{U}\widehat{\mathbf{g}}_{kl}$.

B. Data Transmission with LSFD

During the payload data phase, each AP locally performs an arbitrary receive combining scheme to compute local data estimates. Then, these estimates are gathered and combined at the CPU for final decoding by performing LSFD. More precisely, AP l physically receives the data signals from all UE, which is given by

$$\mathbf{y}^{\mathrm{ul}}_l = \sum\nolimits_{i=1}^{K} \mathbf{h}_{il} s_i + \mathbf{n}_l \tag{8}$$

where $s_i \in \mathbb{C}$ is the signal transmitted by UE i with transmit power $p_i = \mathbb{E}\{|s_i|^2\}$ and $\mathbf{n}_l \sim \mathcal{N}_{\mathbb{C}}(\mathbf{0}, \sigma^2\mathbf{I}_M)$ is the independent

additive receiver noise. We adopt the fractional power control policy [2], [17], where the transmit powers $\{p_k : \forall k\}$ are upper bounded by the maximal transmit power $p_{\max}$.

AP l first transforms the received signal into the angle domain as $\frac{1}{N}\mathbf{U}^{\mathrm{H}}\mathbf{y}_l^{\mathrm{ul}}$ and then selects the local angle domain combining vector $\mathbf{D}_{kl}\mathbf{v}_{kl} \in \mathbb{C}^N$ for UE k to compute the local estimate of s_k as

$$\widehat{s}_{kl} = \frac{1}{N}\mathbf{v}_{kl}^{\mathrm{H}}\mathbf{D}_{kl}\mathbf{U}^{\mathrm{H}}\mathbf{y}_l^{\mathrm{ul}} \tag{9}$$

where $\mathbf{D}_{kl} = \mathbf{I}_N$ if $k \in \mathcal{D}_l$ and $\mathbf{D}_{kl} = \mathbf{0}_N$ otherwise.

In analogy with the *local MMSE (L-MMSE)* combining scheme [2], we propose an angle domain L-MMSE combining scheme that provides the best local data estimate $\widehat{s}_{kl}$ with minimal conditional mean-squared-error (MSE) $\mathbb{E}\{|s_k - \widehat{s}_{kl}|^2|\{\widehat{\mathbf{g}}_{il} : \forall i\}\}$, which is given in the following lemma.

Lemma 1. *At AP l, the local conditional data MSE for UE k is minimized by the angle domain L-MMSE combining vector*

$$\mathbf{v}_{kl} = p_k\left(\sum\nolimits_{i=1}^{K} p_i\left(\widehat{\mathbf{g}}_{il}\widehat{\mathbf{g}}_{il}^{\mathrm{H}} + \mathbf{\Xi}_{il}\right) + \frac{\sigma^2}{N}\mathbf{I}_N\right)^{-1}\mathbf{D}_{kl}\widehat{\mathbf{g}}_{kl}. \tag{10}$$

Proof: This can be proved by computing the conditional expectation and letting $\partial\mathbb{E}\{|s_k - \widehat{s}_{kl}|^2|\{\widehat{\mathbf{g}}_{il} : \forall i\}\}/\partial\mathbf{v}_{kl} = 0$. ∎

Next, the CPU performs the final decoding of s_k by linearly combining $\{\widehat{s}_{kl} : \forall l\}$ forwarded by the APs. We denote by $\mathbf{b}_{ki} = [\mathbf{v}_{k1}^{\mathrm{H}}\mathbf{D}_{k1}\mathbf{g}_{i1}, \ldots, \mathbf{v}_{kL}^{\mathrm{H}}\mathbf{D}_{kL}\mathbf{g}_{iL}]^{\mathrm{T}} \in \mathbb{C}^L$ the angle domain receive-combined channels from UE i when receiving signals from UE k, and $\mathbf{a}_k = [a_{k1}, \ldots, a_{kL}]^{\mathrm{T}} \in \mathbb{C}^L$ the LSFD weight vector of UE k, where $a_{kl} \in \mathbb{C}$ is the weight corresponding to $\widehat{s}_{kl}$. Then, we can obtain the final estimate of s_k as

$$\widehat{s}_k = \sum\nolimits_{l=1}^{L} a_{kl}^{\star}\widehat{s}_{kl} = \sum\nolimits_{i=1}^{K} \mathbf{a}_k^{\mathrm{H}}\mathbf{b}_{ki}s_i + n_k' \tag{11}$$

where $n_k' = \frac{1}{N}\sum_{l=1}^{L} a_{kl}^{\star}\mathbf{v}_{kl}^{\mathrm{H}}\mathbf{D}_{kl}\mathbf{U}^{\mathrm{H}}\mathbf{n}_l$ is the resulting noise. The LSFD vectors $\{\mathbf{a}_k : \forall k\}$ are selected as a deterministic function of the channel statistics at the CPU where the average effective uplink channel $\mathbb{E}\{\mathbf{a}_k^{\mathrm{H}}\mathbf{b}_{kk}\} = \mathbf{a}_k^{\mathrm{H}}\mathbb{E}\{\mathbf{b}_{kk}\}$ is deterministic and non-zero when the aforementioned combining scheme in (10) is selected and employed.

Finally, the achievable uplink SE can be quantified as

$$\mathsf{SE}_k^{\mathrm{ul}} = \frac{\tau_{\mathrm{u}}}{\tau_{\mathrm{c}}}\log_2\left(1 + \mathsf{SINR}_k^{\mathrm{ul}}\right) \quad \text{bit/s/Hz} \tag{12}$$

by using the *hardening bound* [16, Thm. 4.4], where

$$\mathsf{SINR}_k^{\mathrm{ul}} = \frac{p_k|\mathbf{a}_k^{\mathrm{H}}\mathbb{E}\{\mathbf{b}_{kk}\}|^2}{\mathbf{a}_k^{\mathrm{H}}\left(\sum_{i=1}^{K} p_i\mathbb{E}\{\mathbf{b}_{ki}\mathbf{b}_{ki}^{\mathrm{H}}\} - p_k\mathbb{E}\{\mathbf{b}_{kk}\}\mathbb{E}\{\mathbf{b}_{kk}^{\mathrm{H}}\} + \mathbf{F}_k\right)\mathbf{a}_k} \tag{13}$$

is the effective uplink signal-to-interference-plus-noise ratio (SINR) [2, Thm. 5.4] in angle domain with $\mathbf{F}_k = \frac{\sigma^2}{N}\mathrm{diag}(\mathbb{E}\{\|\mathbf{D}_{k1}\mathbf{v}_{k1}\|^2\}, \ldots, \mathbb{E}\{\|\mathbf{D}_{kL}\mathbf{v}_{kL}\|^2\})$. Since $\mathsf{SINR}_k^{\mathrm{ul}}$ in (13) is a generalized Rayleigh quotient of $\mathbf{a}_k$, the optimal angle domain LSFD vector that maximizes $\mathsf{SINR}_k^{\mathrm{ul}}$ is given by

$$\mathbf{a}_k = p_k\left(\sum\nolimits_{i=1}^{K} p_i\mathbb{E}\{\mathbf{b}_{ki}\mathbf{b}_{ki}^{\mathrm{H}}\} + \mathbf{F}_k\right)^{\dagger}\mathbb{E}\{\mathbf{b}_{kk}\} \tag{14}$$

with the help of [16, Lem. B.10] and [16, Lem. B.4]. The resulting maximum SINR value is $\mathsf{SINR}_k^{\mathrm{ul}} = p_k\mathbb{E}\{\mathbf{b}_{kk}^{\mathrm{H}}\}(\sum_{i=1}^{K} p_i\mathbb{E}\{\mathbf{b}_{ki}\mathbf{b}_{ki}^{\mathrm{H}}\} - p_k\mathbb{E}\{\mathbf{b}_{kk}\}\mathbb{E}\{\mathbf{b}_{kk}^{\mathrm{H}}\} + \mathbf{F}_k)^{\dagger}\mathbb{E}\{\mathbf{b}_{kk}\}$.

C. Pilot Assignment with Minimized Normalized MSE

To mitigate the pilot contamination caused by pilot-sharing, we propose an angle domain pilot assignment scheme that improves the channel estimation quality and the resulting SE. In the considered CF system, the collective channel estimate between UE k and its serving APs is formed as $\mathbf{D}_k\widehat{\mathbf{h}}_k = [(\mathbf{D}_{k1}\widehat{\mathbf{h}}_{k1})^{\mathrm{T}}, \ldots, (\mathbf{D}_{kL}\widehat{\mathbf{h}}_{kL})^{\mathrm{T}}]^{\mathrm{T}} \in \mathbb{C}^{LN}$ where $\mathbf{D}_k = \mathrm{diag}(\mathbf{D}_{k1}, \ldots, \mathbf{D}_{kL})$ and $\widehat{\mathbf{h}}_k = [\widehat{\mathbf{h}}_{k1}^{\mathrm{T}}, \ldots, \widehat{\mathbf{h}}_{kL}^{\mathrm{T}}]^{\mathrm{T}}$. Then, the normalized MSE (NMSE) of the channel estimate $\mathbf{D}_k\widehat{\mathbf{h}}_k$ is given by

$$\begin{aligned}\mathsf{NMSE}_k &= \frac{\mathbb{E}\{\|\mathbf{D}_k\mathbf{h}_k - \mathbf{D}_k\widehat{\mathbf{h}}_k\|^2\}}{\mathbb{E}\{\|\mathbf{D}_k\mathbf{h}_k\|^2\}} \\ &= 1 - \frac{\tau_{\mathrm{p}}p_{\mathrm{p}}\sum_{l=1}^{L}\mathrm{tr}(\mathbf{D}_{kl}\mathbf{\Omega}_{kl}\mathbf{U}^{\mathrm{H}}\mathbf{\Psi}_{\iota_k l}^{-1}\mathbf{U}\mathbf{\Omega}_{kl})}{\sum_{l=1}^{L}\mathrm{tr}(\mathbf{D}_{kl}\mathbf{\Omega}_{kl})}.\end{aligned} \tag{15}$$

The pilot contamination is induced by the statistical CSI of the undesired UE contained in $\mathbf{\Psi}_{\iota_k l}$. Therefore, a lower bound of the NMSE in (15) can be obtained if NMSE_k is only related to the statistical CSI of UE k, which is elaborated as follows.

Lemma 2. *Considering a CF M-MIMO system over the angle domain channels, the NMSE in* (15) *is lower bounded by*

$$\underline{\mathsf{NMSE}}_k = 1 - \frac{\tau_{\mathrm{p}}p_{\mathrm{p}}\sum_{l=1}^{L}\mathrm{tr}(\mathbf{D}_{kl}\mathbf{\Omega}_{kl}\mathbf{U}^{\mathrm{H}}\widetilde{\mathbf{\Psi}}_{\iota_k l}^{-1}\mathbf{U}\mathbf{\Omega}_{kl})}{\sum_{l=1}^{L}\mathrm{tr}(\mathbf{D}_{kl}\mathbf{\Omega}_{kl})} \tag{16}$$

where $\widetilde{\mathbf{\Psi}}_{\iota_k l} = \tau_{\mathrm{p}}p_{\mathrm{p}}\mathbf{U}\mathbf{\Omega}_{kl}\mathbf{U}^{\mathrm{H}} + \sigma^2\mathbf{I}_N$. For any l and $i \neq k$, (16) *is achieved when one of the following conditions is satisfied*

1) $\mathbf{D}_{kl}\mathbf{\Omega}_{kl}\mathbf{\Omega}_{il} = \mathbf{0}$,
2) $\mathbf{D}_{kl}\mathbf{\Omega}_{kl}\mathbf{\Omega}_{il} \neq \mathbf{0}$, $\iota_k \neq \iota_i$.

Proof: The details are relegated to Appendix A. ∎

Note that $\mathbf{D}_{kl}\mathbf{\Omega}_{kl}\mathbf{\Omega}_{il} = \mathbf{0}$ occurs when the angle domain channels $\mathbf{g}_{kl}$ and $\mathbf{g}_{il}$ are *non-overlapping* and/or UE k and UE i are not served by AP l simultaneously. To characterize the angle domain overlapping degree when each UE is served by multiple APs, a metric named *similarity* is defined as

$$\rho_{ki} = \frac{\sum_{l=1}^{L}\mathrm{tr}(\mathbf{D}_{kl}\mathbf{\Omega}_{kl}\mathbf{D}_{il}\mathbf{\Omega}_{il})}{\sqrt{\sum_{l=1}^{L}\|\mathbf{D}_{kl}\mathbf{\Omega}_{kl}\|_{\mathrm{F}}^2}\sqrt{\sum_{l=1}^{L}\|\mathbf{D}_{il}\mathbf{\Omega}_{il}\|_{\mathrm{F}}^2}}, \ \forall k, i \tag{17}$$

where $\|\cdot\|_{\mathrm{F}}$ denotes the Frobenious norm. Therefore, an angle domain pilot assignment criterion can be obtained as follows: *For the considered CF M-MIMO system, given each UE is served by multiple APs, the angle domain similarity of UE assigned to the same pilot should be as low as possible.*

Based on the above multiple access criterion, we formulate the following pilot assignment problem,

$$\mathsf{P}_1: \quad \max_{\{\mathcal{S}_\iota : \iota = 1, \ldots, \tau_{\mathrm{p}}\}} \sum\nolimits_{1 \leq \iota < \iota' \leq \tau_{\mathrm{p}}} \sum\nolimits_{i \in \mathcal{S}_\iota, j \in \mathcal{S}_{\iota'}} \rho_{ij} \tag{18}$$

where the overall *inter-set* angle domain similarity is maximized by properly allocating the UE into τ_{p} pilot-sharing sets, i.e., $\mathcal{S}_1, \ldots, \mathcal{S}_{\tau_{\mathrm{p}}}$. In other words, solving P_1 minimizes the overall angle domain similarity of the pilot-sharing UE, implying that the overall pilot contamination is minimized as well. To solve the combinatorial problem P_1, we employ a suboptimal heuristic algorithm [18], which provides an approximate solution as the brute-force approach but in polynomial time. The algorithm proceeds as follows.

1) The first τ_{p} UE are assigned to τ_{p} mutually orthogonal

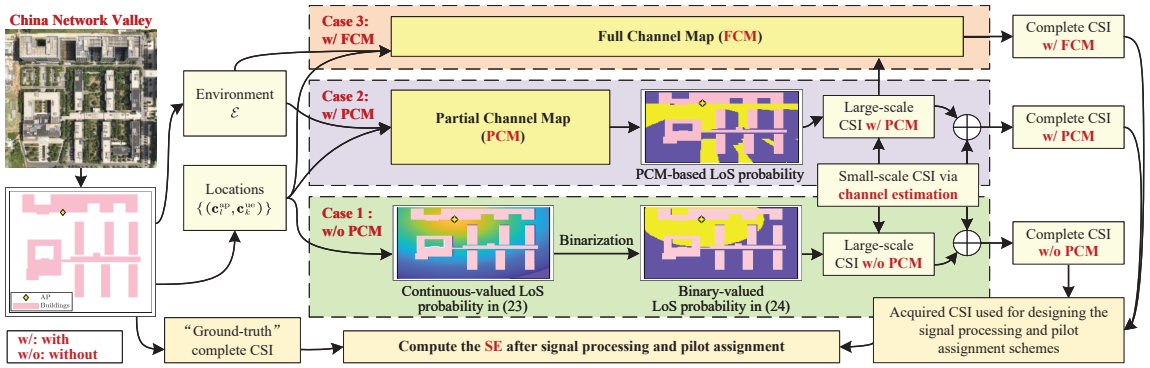

Fig. 2. Procedure of the proposed channel map-based multiple access transmission.

pilots with $|\mathcal{S}_\iota| = 1$, $\forall \iota$.

2) A remaining UE k computes $\rho_k^\iota = \sum_{i \in \mathcal{S}_\iota \cup \{k\}} \rho_{ki}$, $\iota = 1, \ldots, \tau_{\rm p}$ according to (17).
3) Assign UE k to pilot $\iota' = \arg\min_\iota \rho_k^\iota$ and update $\mathcal{S}_{\iota'}$ as $\mathcal{S}_{\iota'} \leftarrow \mathcal{S}_{\iota'} \cup \{k\}$.
4) Repeat steps 2) and 3) until the end of the assignment.

IV. Channel Map-Based Transmission Design

The transmission performance can be further boosted by employing channel maps. Using the channel model in (2), in this section, we propose two channel map-based transmission mechanisms aided by different levels of CSI, namely partial channel map (PCM) and full channel map (FCM), respectively. The procedure is demonstrated in Fig. 2, where the complete channel vectors $\{\mathbf{h}_{kl}\}$ or $\{\mathbf{g}_{kl}\}$ are regarded as the "ground-truth" CSI when computing SE and the acquired CSI obtained with/without channel maps are used for transmission design.

A. Large-Scale CSI-Aware Transmission via PCM

The considered PCM $\mathcal{M}_{\rm PCM}$ can be expressed as a mapping from the current location vectors $(\mathbf{c}_l^{\rm ap}, \mathbf{c}_k^{\rm ue})$ of the desired AP-UE pair (l, k) to the corresponding large-scale CSI $\mathbf{h}_{kl}^{\rm L}$ and $\mathbf{R}_{kl}^{\rm N}$ by the conditional function $f_{\rm PCM}(\cdot|\mathcal{E})$, i.e.,

$$\mathcal{M}_{\rm PCM}: \quad \{\mathbf{h}_{kl}^{\rm L}, \mathbf{R}_{kl}^{\rm N}\} = f_{\rm PCM}((\mathbf{c}_l^{\rm ap}, \mathbf{c}_k^{\rm ue})|\mathcal{E}) \tag{19}$$

where $\mathcal{E}$ represents the *environment* database, which can be constructed by approaches like channel measurements and ray-tracing simulations [19]. More precisely, with the half-wavelength-spaced ULA assumption at each AP, the deterministic LoS component $\mathbf{h}_{kl}^{\rm L}$ is represented as

$$\mathbf{h}_{kl}^{\rm L} = \sqrt{\beta_{kl}^{\rm L}} \left[1, \ldots, e^{\jmath\pi(N-1)\sin(\varphi_{kl})\cos(\theta_{kl})}\right]^{\rm T} \tag{20}$$

where φ_{kl} and θ_{kl} are the azimuth angle of arrival and elevation angle of arrival to UE k seen from AP l, respectively. For the covariance matrix $\mathbf{R}_{kl}^{\rm N}$, we first let $\bar{\varphi}_{kl} = \varphi_{kl} + \delta_\varphi$ and $\bar{\theta}_{kl} = \theta_{kl} + \delta_\theta$ with random deviations $\delta_\varphi \sim \mathcal{N}(0, \sigma_\varphi^2)$ and $\delta_\theta \sim \mathcal{N}(0, \sigma_\theta^2)$, respectively. Then, $\mathbf{R}_{kl}^{\rm N}$ can be generated according to the local scattering model, of which the (m, n)-th element is calculated as [2]

$$[\mathbf{R}_{kl}^{\rm N}]_{mn} = \beta_{kl}^{\rm N} \iint e^{\jmath\pi(m-n)\sin(\bar{\varphi}_{kl})\cos(\bar{\theta}_{kl})} f(\delta_\varphi, \delta_\theta) {\rm d}\delta_\varphi {\rm d}\delta_\theta \tag{21}$$

where $f(\delta_\varphi, \delta_\theta) = \frac{1}{2\pi\sigma_\varphi\sigma_\theta} e^{-\delta_\varphi^2/(2\sigma_\varphi^2)} e^{-\delta_\theta^2/(2\sigma_\theta^2)}$ is the joint probability density function of δ_φ and δ_θ.

The LSF coefficients $\beta_{kl}^{\rm L}$ in (20) and $\beta_{kl}^{\rm N}$ in (21) are obtained based on β_{kl} according to the K-factor κ_{kl} and LoS probability $p_{kl}^{\rm L}$ in (3), where β_{kl} is calculated in dB as [15, Tab. 5.1]

$$\beta_{kl} = \begin{cases} -30.18 - 26\log_{10}\left(\frac{d_{kl}}{1\rm m}\right) + F_{kl}^{\rm L}, & \text{if } p_{kl}^{\rm L} = 1 \\ -34.53 - 38\log_{10}\left(\frac{d_{kl}}{1\rm m}\right) + F_{kl}^{\rm N}, & \text{otherwise} \end{cases} \tag{22}$$

with $F_{kl}^{\rm L} \sim \mathcal{N}(0, 4^2)$ and $F_{kl}^{\rm N} \sim \mathcal{N}(0, 10^2)$ representing the shadow fading in the LoS and NLoS scenarios, respectively.

As illustrated in Fig. 2, the LoS probability $p_{kl}^{\rm L}$ can be obtained through the PCM by employing advanced localization methods [12]. Alternatively, $p_{kl}^{\rm L}$ can be modelled as a distance-related continuous variable [15]

$$p_{kl}^{\rm L} = \begin{cases} \frac{300 - d_{kl}}{300}, & \text{if } 0 < d_{kl} < 300 \\ 0, & \text{otherwise} \end{cases} \tag{23}$$

with $p_{kl}^{\rm L} \in [0, 1]$, which is irrelevant to the practical propagation environment. To convert the range of $p_{kl}^{\rm L}$ in (23) from $[0, 1]$ to $\{0, 1\}$, a parameter $\delta^{\rm L} \in [0, 1]$ is used to approximate the effect of blocking on the LoS probability by controlling the number of LoS paths, denoted as $N_{\rm L}$, in the considered area. As a result, the LoS probability in (23) is rewritten as

$$p_{kl}^{\rm L} = \begin{cases} 1, & \text{if } 0 < d_{kl} < 300(1 - \delta^{\rm L}) \\ 0, & \text{otherwise} \end{cases} \tag{24}$$

which is a binary variable and can be used for calculating the K-factor and the LSF coefficients.

With the environment-related LoS probability, PCM can offer the large-scale CSI that matches the actual wireless channel better than that calculated based on the LoS probability in (24).

B. Small-Scale CSI-Aware Transmission via FCM

The ultimate FCM $\mathcal{M}_{\rm FCM}$ is expected to provide the small-scale CSI $\mathbf{h}_{kl}^{\rm N}$ and $e^{\jmath\phi_{kl}}$ based on the current location vectors $(\mathbf{c}_l^{\rm ap}, \mathbf{c}_k^{\rm ue})$ by the function $f_{\rm FCM}(\cdot|\mathcal{E})$ conditioned on the environment database $\mathcal{E}$. With the available large-scale CSI, the complete channels $\mathbf{h}_{kl}$ and $\mathbf{g}_{kl}$ can be obtained, i.e.,

$$\mathcal{M}_{\rm FCM}: \quad \{\mathbf{h}_{kl}, \mathbf{g}_{kl}\} = f_{\rm FCM}((\mathbf{c}_l^{\rm ap}, \mathbf{c}_u^{\rm ue})|\mathcal{E}). \tag{25}$$

It should be noted that the SE expression in (12) only provides an achievable lower bound of the SE. With the perfect "FCM-aided" CSI $\{\mathbf{g}_{kl} : \forall k, l\}$ obtained through the FCM, an upper bound of the SE can be derived as follows.

Proposition 1. *A SE upper bound of UE k with the perfect "FCM-aided" CSI $\{\mathbf{g}_{kl} : \forall k, l\}$ is*

$$\overline{\rm SE}_k^{\rm ul} = \mathbb{E}\left\{\log_2\left(1 + \overline{\rm SINR}_k^{\rm ul}\right)\right\} \quad \textit{bit/s/Hz} \tag{26}$$

where the SINR is

$$\overline{\rm SINR}_k^{\rm ul} = \frac{p_k |\mathbf{a}_k^{\rm H} \overline{\mathbf{b}}_{kk}|^2}{\mathbf{a}_k^{\rm H} (\sum_{i=1, i\neq k}^{K} p_i \overline{\mathbf{b}}_{ki} \overline{\mathbf{b}}_{ki}^{\rm H} + \overline{\mathbf{F}}_k) \mathbf{a}_k} \tag{27}$$

TABLE I
SYSTEM PARAMETERS.

Parameters	Values	Parameters	Values
L, N	16, 4	K	20
B	20 MHz	τ_{c}, τ_{p}	200, 10
p_{p}, $p_{\max}$	0.1 W, 0.1 W	σ_{φ}, σ_{θ}	10°, 10°

with $\overline{\mathbf{b}}_{ki} = [\mathbf{v}_{k1}^{\mathrm{H}}\mathbf{D}_{k1}\mathbf{g}_{i1}, \ldots, \mathbf{v}_{kL}^{\mathrm{H}}\mathbf{D}_{kL}\mathbf{g}_{iL}]$ *and* $\overline{\mathbf{F}}_k = \frac{\sigma^2}{N}\mathrm{diag}(\|\mathbf{D}_{k1}\mathbf{v}_{k1}\|^2, \ldots, \|\mathbf{D}_{kL}\mathbf{v}_{kL}\|^2)$.

Proof: We first rewrite the final estimate $\widehat{s}_k$ in (11) as

$$\widehat{s}_k = \mathbf{a}_k^{\mathrm{H}}\mathbf{b}_{kk}s_k + \sum\nolimits_{i=1, i\neq k}^{K} \mathbf{a}_k^{\mathrm{H}}\mathbf{b}_{ki}s_i + n'_k \tag{28}$$

where the first term is the desired signal obtained over a known channel. Then, the proof follows a similar approach as in [2, Coro. 5.10] by combining interference and noise in one term, but with angle domain receive-combined channels $\{\overline{\mathbf{b}}_{ki} : \forall k, i\}$ and combining vectors $\{\mathbf{v}_{kl} : \forall k, l\}$. ∎

Similar to (14), the generalized Rayleigh quotient of $\overline{\mathsf{SINR}}_k^{\mathrm{ul}}$ in (27) allows computing the best LSFD vector $\overline{\mathbf{a}}_k^{\mathrm{opt}}$ that maximizes $\overline{\mathsf{SINR}}_k^{\mathrm{ul}}$, which is given as follows.

Corollary 1. *The effective SINR in* (27) *is maximized by*

$$\overline{\mathbf{a}}_k = p_k \left(\sum\nolimits_{i=1}^{K} p_i \overline{\mathbf{b}}_{ki}\overline{\mathbf{b}}_{ki}^{\mathrm{H}} + \overline{\mathbf{F}}_k \right)^{\dagger} \overline{\mathbf{b}}_{kk} \tag{29}$$

which leads to $\overline{\mathsf{SINR}}_k^{\mathrm{ul}} = p_k \overline{\mathbf{b}}_{kk}^{\mathrm{H}} (\sum_{i=1}^{K} p_i \overline{\mathbf{b}}_{ki}\overline{\mathbf{b}}_{ki}^{\mathrm{H}} + \overline{\mathbf{F}}_k)^{\dagger} \overline{\mathbf{b}}_{kk}$.

Proof: The proof follows the results in [16, Lem. B.10] and [16, Lem. B.4]. ∎

Proposition 1 is applicable to any receive combining vector $\mathbf{v}_{kl}$ and any channel model, including the one in (2) and the 6GPCM. We derive the MMSE-type combining scheme with interference suppression capability, which is given as follows.

Lemma 3. *At AP l with perfect angle domain CSI $\{\mathbf{g}_{il} : \forall i\}$, the local conditional data MSE $\mathbb{E}\{|s_k - \widehat{s}_{kl}|^2 | \{\mathbf{g}_{il} : \forall i\}\}$ for UE k is minimized by the angle domain L-MMSE combiner*

$$\overline{\mathbf{v}}_{kl} = p_k \left(\sum\nolimits_{i=1}^{K} p_i \mathbf{g}_{il}\mathbf{g}_{il}^{\mathrm{H}} + \frac{\sigma^2}{N}\mathbf{I}_N \right)^{-1} \mathbf{D}_{kl}\mathbf{g}_{kl}. \tag{30}$$

Proof: The proof is similar as in Lemma 1 but with the local conditional data MSE $\mathbb{E}\{|s_k - \widehat{s}_{kl}|^2 | \{\mathbf{g}_{il} : \forall i\}\}$. ∎

V. RESULTS AND ANALYSIS

In this section, we will evaluate our proposed angle domain multiple access schemes and the transmission design using FCM and PCM. As illustrated in Fig. 1, we consider an urban microcell scenario with buildings mimicking the exterior dimensions and layouts of the China Network Valley, Nanjing, China. There are L APs mounted on the rooftops of the buildings offering an adequate network coverage, and K UE uniformly distributed in a 318×330 m^2 area. Each AP serves τ_{p} UE with the strongest channels. Unless otherwise specified, the adopted system parameters are given in Table I. PCM is used for large-scale channel statistics by default. SE values are calculated according to (12) with the channel model in (2).

We propose two angle domain schemes, namely "P-Angle" and "F-Angle", where the L-MMSE combining and optimal LSFD are used. P-Angle performs pilot assignment by solving P_1 in (18), whereas F-Angle requires no pilot assignment since channel estimation is obviated using the FCM. Two space domain benchmark schemes are considered for comparison, namely "Weighted [4]" and "Random", as detailed in Table II. When neither FCM nor PCM is utilized, the large-scale channel statistics used for channel estimation are obtained with the LoS probability computed according to (24).

TABLE II
THE CONSIDERED MULTIPLE ACCESS SCHEMES.

Schemes	Domain	Pilot Assignment
F-Angle	Angle	–
P-Angle		Obtained by solving P_1 in (18)
Weighted [4]	Space	Heuristic scheme [4]
Random		Random assignment

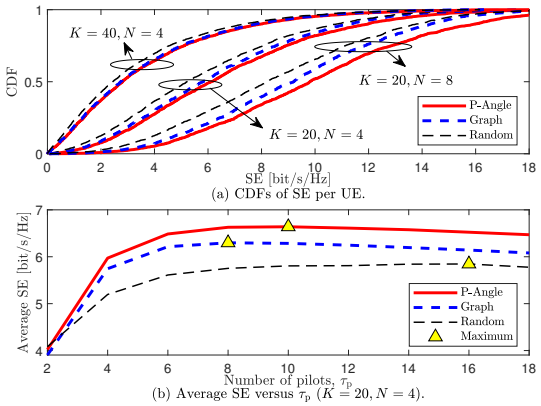

(a) CDFs of SE per UE.

(b) Average SE versus τ_{p} ($K = 20, N = 4$).

Fig. 3. (a) CDFs of SE per UE considering different combinations of K and N and (b) average SE versus τ_{p} when $K = 20, N = 4$.

Fig. 3 evaluates the SE performance of our proposed angle domain multiple access transmission design. Fig. 3 (a) depicts the cumulative distribution functions (CDFs) of SE per UE, where P-Angle is observed to outperform the benchmark in the considered cases. This is expected, since the UE similarity is revealed more prominently in the angle domain, which implies better pilot assignment for interference suppression. Moreover, the case of $K = 20, N = 4$ outperforms the case of $K = 40, N = 4$ thanks to the reduced inter-UE interference by having fewer serving UE. The case of $K = 20, N = 8$ further improves the average SE due to the enhanced interference suppression gain by having more antennas per AP. In Fig. 3 (b), we observe that the average SE is a concave function of τ_{p}, since increasing τ_{p} not only promotes the SINR but also reduces the prelog factor $\frac{\tau_{\mathrm{u}}}{\tau_{\mathrm{c}}} = 1 - \frac{\tau_{\mathrm{p}}}{\tau_{\mathrm{c}}}$ in (12).

Fig. 4 focuses on the channel map-based transmission design. For a fair comparison, the LoS probabilities in both cases with and without PCM are held constant. In Fig. 4 (a), P-Angle outperforms Weighted in both cases, with higher SE when using PCM due to the *a priori* large-scale channel statistics. F-Angle further enhances SE by utilizing perfect FCM-aided CSI. F-Angle (6GPCM) achieves a similar average SE to F-Angle but offers a 25.0% higher 95%-likely SE, indicating that channel realizations modeled by 6GPCM are more uniform than those from (2). Fig. 4 (b) shows the effect of the number of LoS paths, N_{L}, on average SE, where $N_{\mathrm{L}} \in [0, 320]$ with $L = 16, K = 20$. We consider a case labeled "Appr", where the *approximate* "ground-truth" CSI is obtained using the LoS probability from (24). As depicted in Fig. 4 (b), average SE

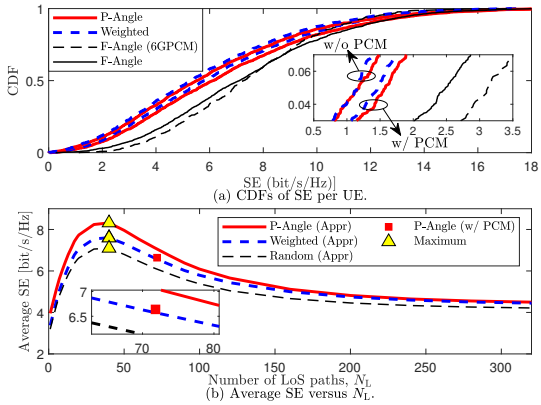

Fig. 4. (a) CDFs of SE per UE and (b) average SE versus N_{L}, considering different channel maps.

is a concave function of N_{L}. This occurs since weak received signal strength is observed when LoS paths are absent, while excessive LoS paths cause undesirable interference between UE, both reducing average SE. By comparing P-Angle (w/ PCM) with P-Angle (Appr) at $N_{\mathrm{L}} = 71.8$, the average N_{L} for the scenario, we find that P-Angle (Appr) achieves a higher average SE than P-Angle (w/ PCM). This results from the weaker overall signal strength in the PCM case caused by building blockage, which increases the average distance of the LoS paths while keeping N_{L} constant. Therefore, the actual propagation environment must be considered in transmission design to avoid overestimating achievable SE performance.

VI. Conclusions

This paper has proposed a channel map-based angle domain multiple access scheme for uplink CF M-MIMO communications. It includes a two-stage data reception and pilot assignment scheme that incorporates angle domain MMSE-type receive combining and LSFD vectors to reduce overall interference. Simulation results have shown significant enhancements in SE performance compared to space domain alternatives. Furthermore, two channel map-based transmission mechanisms aided by PCM and FCM have been constructed, featuring a tailored data reception scheme with a newly derived upper-bound SE expression and combining and LSFD vectors. The results have indicated that channel map-based schemes outperform those without channel maps, confirming the advantages of channel awareness and effective CSI exploitation.

Acknowledgment

This work was supported by the National Natural Science Foundation of China (NSFC) under Grants 62394290, 62394291, and 62401643, the Fundamental Research Funds for the Central Universities under Grant 2242022k60006, the Young Elite Scientists Sponsorship Program by China Association for Science and Technology under Grant 2022QNRC001, and the Research Fund of National Mobile Communications Research Laboratory, Southeast University, under Grant 2025A05.

Appendice A

According to the definitions of NMSE_k and $\widetilde{\boldsymbol{\Psi}}_{\iota_k l}$, we have

$$\mathrm{tr}\left(\mathbf{D}_{kl}\boldsymbol{\Omega}_{kl}\mathbf{U}^{\mathrm{H}}\boldsymbol{\Psi}_{\iota_k l}^{-1}\mathbf{U}\boldsymbol{\Omega}_{kl}\right) \tag{31}$$

$$=\mathrm{tr}(\mathbf{D}_{kl}\boldsymbol{\Omega}_{kl}\mathbf{U}^{\mathrm{H}}(\widetilde{\boldsymbol{\Psi}}_{\iota_k l}+\widetilde{\boldsymbol{\Omega}}_{kl}^{\mathrm{res}})^{-1}\mathbf{U}\boldsymbol{\Omega}_{kl}) \tag{32}$$

$$\leq\mathrm{tr}(\mathbf{U}\boldsymbol{\Omega}_{kl}\mathbf{D}_{kl}\boldsymbol{\Omega}_{kl}\mathbf{U}^{\mathrm{H}}\widetilde{\boldsymbol{\Psi}}_{\iota_k l}^{-1}) \tag{33}$$

with the help of the results in [2, Lem. B.4], where $\widetilde{\boldsymbol{\Omega}}_{kl}^{\mathrm{res}} = \tau_{\mathrm{p}}p_{\mathrm{p}}\sum_{i\in\mathcal{S}_{\iota_k}\setminus\{k\}}\mathbf{U}\boldsymbol{\Omega}_{il}\mathbf{U}^{\mathrm{H}}$ and the equality occurs when $\widetilde{\boldsymbol{\Omega}}_{kl}^{\mathrm{res}}\widetilde{\boldsymbol{\Psi}}_{\iota_k l}^{-1}\mathbf{U}\boldsymbol{\Omega}_{kl}\mathbf{D}_{kl}\boldsymbol{\Omega}_{kl}\mathbf{U}^{\mathrm{H}} = \mathbf{0}$. With the results in [16, Lem. B.4], we rewrite the above condition as

$$\tau_{\mathrm{p}}p_{\mathrm{p}}\sum_{i\in\mathcal{S}_{\iota_k}\setminus\{k\}}\mathbf{U}\mathbf{D}_{kl}\boldsymbol{\Omega}_{il}\boldsymbol{\Omega}_{kl}\left(\tau_{\mathrm{p}}p_{\mathrm{p}}\boldsymbol{\Omega}_{kl}+\frac{\sigma^2}{N}\mathbf{I}_N\right)^{-1}\boldsymbol{\Omega}_{kl}\mathbf{U}^{\mathrm{H}}=\mathbf{0}$$

which holds when one of the conditions in Lemma 2 is satisfied. This completes the proof.

References

[1] C.-X. Wang, *et al.*, "On the road to 6G: Visions, requirements, key technologies, and testbeds," *IEEE Commun. Surveys Tuts.*, vol. 25, no. 2, pp. 905–974, 2nd Quart. 2023.

[2] Ö. T. Demir, E. Björnson, and L. Sanguinetti, "Foundations of user-centric cell-free massive MIMO," *Foundations and Trends® in Signal Processing*, vol. 14, no. 3–4, pp. 162–472, 2021.

[3] S. Chen, J. Zhang, E. Björnson, Ö. T. Demir, and B. Ai, "Energy-efficient cell-free massive MIMO through sparse large-scale fading processing," *IEEE Trans. Wireless Commun.*, vol. 22, no. 12, pp. 9374–9389, Dec. 2023.

[4] W. Zeng, Y. He, B. Li, and S. Wang, "Pilot assignment for cell-free massive MIMO systems using a weighted graphic framework," *IEEE Trans. Veh. Tech.*, vol. 70, no. 6, pp. 6190–6194, June 2021.

[5] A. Al Ayidh, Y. Sambo, and M. A. Imran, "Mitigation pilot contamination based on matching technique for uplink cell-free massive MIMO systems," *Sci. Rep.*, vol. 12, no. 1, p. 16893, 2022.

[6] R. Feng, C.-X. Wang, J. Huang, X. Gao, S. Salous, and H. Haas, "Classification and comparison of massive MIMO propagation channel models," *IEEE Internet J.*, vol. 9, no. 23, pp. 23 452–23 471, Dec. 2022.

[7] J. Yang, A.-A. Lu, Y. Chen, X. Gao, X.-G. Xia, and D. T. Slock, "Channel estimation for massive MIMO: An information geometry approach," *IEEE Trans. Signal Process.*, vol. 70, pp. 4820–4834, Oct. 2022.

[8] H. Chang, *et al.*, "A novel 3D beam domain channel model for UAV massive MIMO communications," *IEEE Trans. Wireless Commun.*, vol. 22, no. 8, pp. 5431–5445, Aug. 2023.

[9] C.-X. Wang, J. Huang, H. Wang, X. Gao, X. You, and Y. Hao, "6G wireless channel measurements and models: Trends and challenges," *IEEE Veh. Technol. Mag.*, vol. 15, no. 4, pp. 22–32, Dec. 2020.

[10] C.-X. Wang, Z. Lv, X. Gao, X. You, Y. Hao, and H. Haas, "Pervasive wireless channel modeling theory and applications to 6G GBSMs for all frequency bands and all scenarios," *IEEE Trans. Veh. Technol.*, vol. 71, no. 9, pp. 9159–9173, Sept. 2022.

[11] C.-X. Wang, Z. Lv, Y. Chen, and H. Haas, "A complete study of space-time-frequency statistical properties of the 6G pervasive channel model," *IEEE Trans. Commun.*, vol. 71, no. 12, pp. 7273–7287, Dec. 2023.

[12] Y. Zeng, *et al.*, "A tutorial on environment-aware communications via channel knowledge map for 6G," *IEEE Commun. Surveys Tuts.*, vol. 26, no. 3, pp. 1478–1519, 3rd Quart. 2024.

[13] D. Wu, Y. Zeng, S. Jin, and R. Zhang, "Environment-aware hybrid beamforming by leveraging channel knowledge map," *IEEE Trans. Wireless Commun.*, vol. 23, no. 5, pp. 4990–5005, May 2023.

[14] H. Li, P. Li, J. Xu, J. Chen, and Y. Zeng, "Derivative-free placement optimization for multi-UAV wireless networks with channel knowledge map," in *Proc. IEEE ICC'22 Workshops*, Seoul, Korea, Republic of, June 2022, pp. 1029–1034.

[15] *Spatial Channel Model for Multiple Input Multiple Output (MIMO) simulations (Release 18)*, document TR 25.996, V18.0.0, 3GPP, Mar. 2024.

[16] E. Björnson, J. Hoydis, and L. Sanguinetti, "Massive MIMO networks: Spectral, energy, and hardware efficiency," *Foundations and Trends® in Signal Processing*, vol. 11, no. 3–4, pp. 154–655, 2017.

[17] S. Chen, J. Zhang, E. Björnson, J. Zhang, and B. Ai, "Structured massive access for scalable cell-free massive MIMO systems," *IEEE J. Sel. Areas Commun.*, vol. 39, no. 4, pp. 1086–1100, Apr. 2021.

[18] S. Sahni and T. Gonzalez, "P-complete approximation problems," *J. ACM*, vol. 23, no. 3, pp. 555–565, July 1976.

[19] T. Qi, C. Huang, J. Shi, J. Li, S. Chen, and C.-X. Wang, "A novel dynamic channel map for 6G MIMO communications," in *Proc. IEEE/CIC ICCC'24*, Hangzhou, China, Aug. 2024, pp. 809–814.